IEEE Access
Multidisciplinary | Rapid Review | Open Access Journal

Received March 9, 2020, accepted March 17, 2020, date of publication March 19, 2020, date of current version March 31, 2020.

Digital Object Identifier 10.1109/ACCESS.2020.2982040

Positioning and Sequence Planning of Drilling Boreholes in Hard Rock Roadway

YUMING CUI[1,2], (Member, IEEE), SONGYONG LIU[1,2], HUIFU JI[1,2], YUHUI HAN[1,2], AND YUESHEN YU[1,3]

[1]School of Mechatronic Engineering, China University of Mining and Technology, Xuzhou 221116, China
[2]Jiangsu Collaborative Innovation Center of Intelligent Mining Equipment, China University of Mining and Technology, Xuzhou 221008, China
[3]School of Electrical and Power Engineering, China University of Mining and Technology, Xuzhou 221116, China

Corresponding author: Songyong Liu (lsycumt@ 163.com)

This work was supported in part by the National Natural Science Foundation of China under Grant 51975570, in part by the Xuzhou Science and Technology Plan Project under Grant KC19244, in part by the Top-notch Academic Programs Project of Jiangsu Higher Education Institutions (TAPP), and in part by the Priority Academic Program Development of Jiangsu Higher Education Institutions (PAPD).

ABSTRACT The safety and efficiency of hard rock roadway excavation are the two sides of a coin limiting the implementation of roadway construction. It is an effective way to improve the performance in hard rock tunneling to effectively release the internal stress in rock mass by arranging pre-prepared boreholes in rock section. In order to improve the rock breaking performance and tunneling efficiency, we analyze the borehole positioning accuracy and explore boreholes sequence planning problem in hard rock excavation simulatively and experimentally. The kinematics model of drilling mechanism is established based on the D-H method. RBF neural network algorithm is adopted to accurately position borehole. The results show that accuracy of simulated borehole positioning is controlled at 1.5% while the accuracy is 5.6% of experiment. The Ant Colony Algorithm (ACA) is employed to optimize the sequence planning of drilling boreholes with the optimization goals of minimum moving distance and minimum swing angle separately. Simulation results show that rock-drilling with the minimum swing angle produces smaller positioning deviation and higher efficiency, which is a practical automatic roadway borehole drilling method.

INDEX TERMS Borehole positioning, RBF neural network, sequence planning, ant colony algorithm (ACA).

I. INTRODUCTION

Drilling-blasting method, comprehensive mechanized excavation and TBM (Tunnel Boring Machine) method are the three main methods for roadway excavation in underground coal mining [1]. TBM method has a higher cost and longer preparation time, and comprehensive mechanized excavation cannot excavate hard rock (f>8) effectively, while the drilling-blasting method has a superior adaptability to different rock region and hardness. With the increase of mining depth in tunnels and roadways, rock hardness generally exceeds the economic cutting capability (100 MPa) of mechanical tools [2], [3]. Drilling-blasting method can be used to excavate hard roadways, but the roadway section and the safety are poorly controlled. Thus, non-blasting mining methods, including water jet and drilling-fracturing, have been investigated and tested [4]–[7]. In 1965, the British Farmer, I. W. *et al.* studied the impact erosion effects on the non-igneous rock fracture by pure water jets experimentally and analyzed the rock-breaking mechanism [8]. Scholars at home and abroad have conducted a thorough study on rock breaking by water jet from the aspects of jet type, nozzle structure, rock-breaking mechanism, crack propagation, specific energy consumption [9]–[12]. These combined the applications of water jet in hard rock excavation points out the feasibility of water jet method. Hard rock (>100MPa) water jet excavation requires excellent sealing performance of equipment, large amount of water supply and power-matching resulting in huge energy loss [13]. The drilling-fracturing method is a new method which combines traditional drilling-blasting and with fracturing technology. Prefabricated boreholes are arranged on the working face by rock drill, and the rock is broken under the fracturing force. According to the advantages of controllability of

The associate editor coordinating the review of this manuscript and approving it for publication was Junhua Li.

roadway formation and high excavation efficiency, the feasibility and effectiveness of drilling-fracturing method has been proved [4], [14]–[17]. In the process of hard rock roadway drilling and excavating, the unloading effect is generated due to the transient release of high natural geostress. Rock disintegration with uncertain lumpiness is produced after explosive blasting [18]. The roadway will be seriously over-excavated or under-excavated resulting in the roadway section shape can not meet the construction requirements [19]. Subsequent separate grouting support and roadway repair work is needed and affects the construction progress [20]. Therefore, positioning accuracy of borehole directly determines crack propagation direction and roadway section flatness, while reasonable borehole sequence can effectively reduce energy consumption and improve roadway excavation efficiency. Therefore, it is necessary to investigate and control borehole positioning and sequence planning [21]. For boreholes positioning technology, Wu proposed a novel positioning method based on binocular stereoscopic vision and calculated the three-dimensional position of boreholes by the triangulation method [22]. The positioning error was within 25mm by experiment. Zhang *et al.* [23], Pirinen *et al.* [24] all adopted the PID method to control the drilling jumbos and established motion model of drilling-rod by rotation theory. Compared with manual control, the automatic positioning method can control the position error within 6.5 cm, and short the positioning time greatly. For boreholes sequence planning technology, Andersson K carried out simulation research with the load as an optimization objective [25]. Wu Wan Rong simplified the drilling sequence planning to a 3-TSP problem, established the optimization function of minimum moving distance, and then solved the TSP problem by using the adaptive genetic algorithm [26]. In addition, RBF is mostly used for parameter setting of motion controller and smooth control of robot motion path [27]–[32]. ACA (ACO) is used for path optimization and obstacle avoidance planning for robots or UAVs [33]–[39]. Variants of ACA reduce the computing costs and training speeds [28], [40], [41].

At present, manual estimation has not been replaced by automatic drilling positioning and borehole sequence planning in mining drilling equipment. The positioning error of drilling-rod can not be effectively simulated and controlled without the effective inverse kinematics of drilling jumbo mechanism. Reasonable optimization targets and mature optimization methods of borehole positioning and sequence planning have not been summarized in the existing investigations on in hard rock excavation. Based on the kinematic model of drilling-rod, the borehole positioning and sequence planning in hard rock roadway is realized by RBF neural network algorithm and ant colony algorithm. In order to precisely positioning hole and improve drilling efficiency, the authors cooperated with enterprise to explore the application of RBF and ACA in hard rock drilling positioning and hole sequence planning and field experiment were carried out subsequent. Simulated and experimental research were carried out to verify the technological feasibility in engineering application. Both laboratory and field experiments showed that it is feasible using RBF and ACA to improve drilling positioning and efficiency compared with manual drilling.

II. KINEMATICS MODEL

A. MECHANICAL STRUCTURE

The physical diagram of drilling mechanism in drilling jumbo is illustrated in Figure 1. Kinematic pairs of the drilling mechanism consist of a slip compensation pair and five rotating pairs including drilling-rod swing mechanism, drilling-rod swing compensation mechanism, drilling-rod lifting mechanism, drilling-rod lifting compensation mechanism and overturning mechanism, with six degrees of freedom. The slip, lifting and swinging of drilling mechanism are driven by hydraulic cylinders, while the overturning motion is realized by worm gear and worm mechanism. The swing mechanism and overturning mechanism compensate each other to ensure the drilling-rod perpendicular to the working section.

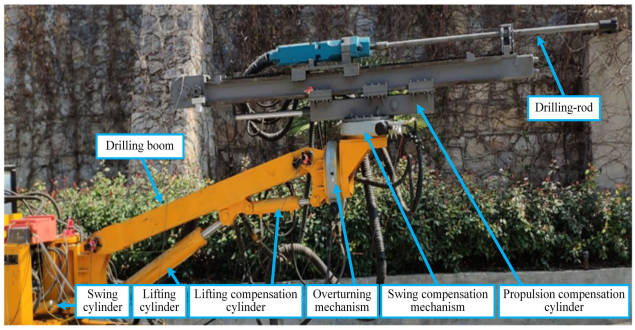

FIGURE 1. Physical diagram of drilling mechanism with 6 degrees of freedom.

B. SPATIAL PARAMETRIC MODEL

The spatial model and parametric coordinate system is abstracted established by D-H (Denavit-Hartenberg) method, as shown in Figure 2.

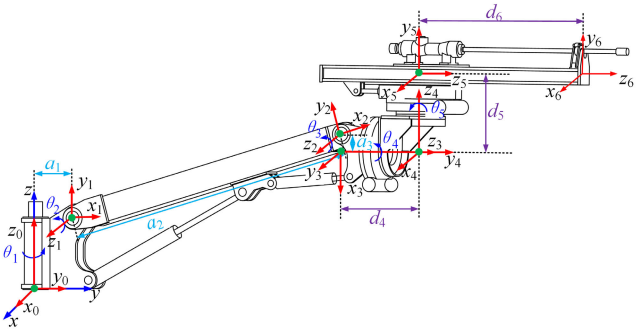

FIGURE 2. Spatial model of the drilling mechanism.

Model parameters can be defined sequentially from the definition method of D-H coordinate system as follows, and presented in Table 1.

β_i is the rotation angle around the x_{i-1} axis;
a_i is the moving distance along the x_{i-1} axis;
d_i is the moving distance along the z_{i-1} axis;
θ_i is the rotation angle around the z_{i-1} axis.

Therefore, the pose transformation matrix between any adjacent parametric coordinate systems i and $i+1$ can be expressed as

$$ {}^{i}_{i+1}T = \begin{bmatrix} c\theta_{i+1} & -s\theta_{i+1}c\alpha_{i+1} & s\theta_{i+1}s\alpha_{i+1} & a_{i+1}c\theta_{i+1} \\ s\theta_{i+1} & c\theta_{i+1}c\alpha_{i+1} & -c\theta_{i+1}s\alpha_{i+1} & a_{i+1}s\theta_{i+1} \\ 0 & s\alpha_{i+1} & c\alpha_{i+1} & d_{i+1} \\ 0 & 0 & 0 & 1 \end{bmatrix} \tag{1} $$

where $c\theta$, $s\theta$, $c\alpha$, $s\alpha$ denote $\cos\theta$, $\sin\theta$, $\cos\alpha$, $\sin\alpha$, respectively.

The general pose transformation matrix of drilling mechanism from the initial coordinate system $o_0x_0y_0z_0$ to the terminal coordinate system $o_6x_6y_6z_6$ is expressed as

$$ {}^{0}_{6}T = {}^{0}_{1}T{}^{1}_{2}T{}^{2}_{3}T{}^{3}_{4}T{}^{4}_{5}T{}^{5}_{6}T \tag{2} $$

Substituting the parameters in TABLE 1 into (1) and (2), the following result is obtained

$$ {}^{0}_{6}T = \begin{bmatrix} n_x & o_x & a_x & p_x \\ n_y & o_y & a_y & p_y \\ n_z & o_z & a_z & p_z \\ 0 & 0 & 0 & 1 \end{bmatrix} \tag{3} $$

where $\mathbf{n} = [n_{6x}, n_{6y}, n_{6z}]^T$, $\mathbf{o} = [o_{6x}, o_{6y}, o_{6z}]^T$, $\mathbf{a} = [a_{6x}, a_{6y}, a_{6z}]^T$ are the direction vectors projected from the terminal coordinate system $o_6x_6y_6z_6$ to the initial coordinate system $o_0x_0y_0z_0$, respectively. $\mathbf{p} = [p_{6x}, p_{6y}, p_{6z}]^T$ is the position vector projected from $o_6x_6y_6z_6$ to $o_0x_0y_0z_0$. The specific calculation formulas of the parameters above are as follows.

$$ \begin{cases} n_x = -c\theta_5(s\theta_1s\theta_4 + c\theta_4(c\theta_1s\theta_2s\theta_3 - c\theta_1c\theta_2c\theta_3)) \\ -s\theta_5(c\theta_1c\theta_2s\theta_3 + c\theta_1c\theta_3s\theta_2) \\ n_y = c\theta_5(c\theta_1s\theta_4 - c\theta_4(s\theta_1s\theta_2s\theta_3 - s\theta_1c\theta_2c\theta_3)) \\ -s\theta_5(s\theta_1c\theta_2s\theta_3 + s\theta_1s\theta_2s\theta_3) \\ n_z = s\theta_5(c\theta_2c\theta_3 - s\theta_2s\theta_3) + c\theta_4c\theta_5(c\theta_2s\theta_3 + c\theta_3s\theta_2) \\ o_x = s\theta_4(c\theta_1s\theta_2s\theta_3 - c\theta_1c\theta_2c\theta_3) - c\theta_4s\theta_1 \\ o_y = c\theta_1c\theta_4 + s\theta_4(s\theta_1s\theta_2s\theta_3 - s\theta_1c\theta_2c\theta_3) \\ o_z = -s\theta_4(c\theta_2s\theta_3 + c\theta_3s\theta_2) \\ a_x = s\theta_5(s\theta_1s\theta_4 + c\theta_4(c\theta_1s\theta_2s\theta_3 - c\theta_1c\theta_2c\theta_3)) \\ -c\theta_5(c\theta_1c\theta_2c\theta_3 + c\theta_1c\theta_3s\theta_2) \\ a_y = -s\theta_5(c\theta_1s\theta_4 - c\theta_4(s\theta_1s\theta_2s\theta_3 - s\theta_1s\theta_2c\theta_3)) \\ -c\theta_5(s\theta_1c\theta_2s\theta_3 + s\theta_1c\theta_3s\theta_2) \\ a_z = c\theta_5(c\theta_2c\theta_3 - s\theta_2s\theta_3) - c\theta_4s\theta_5(c\theta_2s\theta_3 + c\theta_3s\theta_2) \\ p_x = 350c\theta_1 + d_6(s\theta_5(s\theta_1s\theta_4 + c\theta_4(c\theta_1s\theta_2s\theta_3 - c\theta_1c\theta_2c\theta_3)) \\ -c\theta_5(c\theta_1c\theta_2c\theta_3 + c\theta_1c\theta_3s\theta_2)) + 2200c\theta_1c\theta_2 + 500c\theta_4s\theta_1 \\ \quad -500s\theta_4(c\theta_1s\theta_2s\theta_3 - c\theta_1c\theta_2c\theta_3) - 115c\theta_1s\theta_2s\theta_3 \\ +115c\theta_1c\theta_2c\theta_3 - 543c\theta_1c\theta_2s\theta_3 - 543c\theta_1c\theta_3s\theta_2 \\ p_y = 350s\theta_1 + d_6(s\theta_5(c\theta_1s\theta_4 - c\theta_4(s\theta_1s\theta_2s\theta_3 - s\theta_1c\theta_1c\theta_3)) \\ +c\theta_5(s\theta_1c\theta_2s\theta_3 + s\theta_1c\theta_3s\theta_2)) + 2200c\theta_1c\theta_2 - 500c\theta_4c\theta_1 \\ \quad -500s\theta_4(s\theta_1s\theta_2s\theta_3 - s\theta_1c\theta_2c\theta_3) - 115s\theta_1s\theta_2s\theta_3 \\ +115s\theta_1c\theta_2c\theta_3 - 543s\theta_1c\theta_2s\theta_3 - 543s\theta_1c\theta_3s\theta_2 \\ p_z = 350s\theta_1 + d_6(c\theta_5(c\theta_2c\theta_3 - s\theta_2s\theta_3) \\ -c\theta_4s\theta_5(c\theta_2s\theta_3 + c\theta_3s\theta_2)) + c\theta_5(s\theta_1c\theta_2s\theta_3 + s\theta_1c\theta_3s\theta_2)) \\ +2200s\theta_2 + 500s\theta_4(c\theta_2s\theta_3 - s\theta_2c\theta_3) + 115c\theta_2s\theta_3 \\ +115s\theta_2c\theta_3 + 543c\theta_2c\theta_3 - 543s\theta_3s\theta_2 \end{cases} \tag{4} $$

TABLE 1. Parameters and their scopes of drilling mechanism.

Coordinate system	Swing angle			Parameters		
	θ	Max /°	Min /°	β /°	a /mm	d /mm
$x_1y_1z_1$	θ_1	45	-45	90	350	/
$x_2y_2z_2$	θ_2	56	-16	90	2200	/
$x_3y_3z_3$	θ_3	-75	-135	-90	115	/
$x_4y_4z_4$	θ_4	180	-180	90	/	543
$x_5y_5z_5$	θ_5	90	-90	-90	/	500
$x_6y_6z_6$	d_6	2100	1500	0	/	d_6

III. METHODOLOGY

A. DRILLING-ROD POSITIONING CONTROL

Accurate positioning of drilling-rod is the basis of adaptive rock drilling control in roadway excavation. Based on the known borehole position and the spatial model of the drilling mechanism, we proposed a variable value optimization method to inversely calculate the optimal value of every joint variable based on RBF neural network, the so called inverse kinematics solution of the rock drilling mechanism.

RBF neural network is a three-layer neural network, which includes input layer, hidden layer and output layer. The transformation from the input layer to the hidden layer space is nonlinear, while linearization is applied in the transformation from the hidden layer space to the output layer space. In this paper, joint variables, expressed as follows, are regarded as the output layer.

$$ T = [\theta_1, \theta_2, \theta_3, \theta_4, \theta_5, d_6] \tag{5} $$

${}^{0}_{6}T$, the determined general pose transformation matrix of drilling mechanism, is treated as the input layer of RBF neural network by bring the offered borehole coordinates into (3). It is difficult to ensure the 12 parameters in the general pose transformation matrix to be orthogonal strictly. Hence, Euler transform RPY is employed to propose a new input matrix reducing the required variables.

$$ P_T = \left[p_x, p_y, p_z, \alpha, \beta, \gamma\right] \tag{6} $$

The corresponding transformation formula is presented as follows.

$$ \begin{cases} \alpha = \text{a tan } 2(n_y, n_x) \\ \beta = \text{a tan } 2(-n_z, n_x\cos\alpha + n_y\sin\alpha) \\ \gamma = \text{a tan } 2(a_x\sin\alpha - a_y\cos\alpha, -o_x\sin\alpha + o_y\cos\alpha) \end{cases} \tag{7} $$

The input data are linearized and projected into the [0, 1] by Min-Max Normalization method avoiding the singular value and the linear conversion function is shown below.

$$ P'_T[i] = \frac{P_T[i] - \min P_T[i]}{\max P_T[i] - \min P_T[i]} \tag{8} $$

where $P'_T[i]$ is the normalized input matrix.

The kinematic inverse solution of the drill mechanism is obtained based on the mechanism model parameters and RBF network, and the correctness and practicability is verified by simulation and experiment. The main process of drilling positioning control parameters determined by RBF neural network is shown in the Figure 3 below.

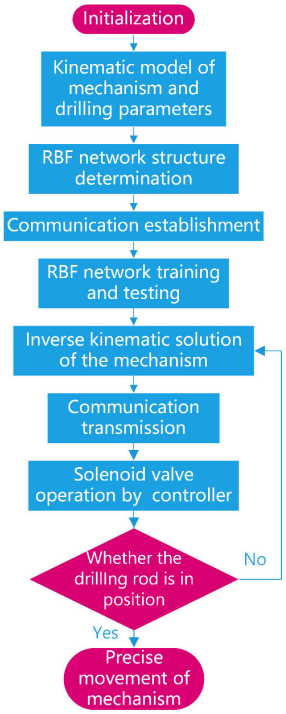

FIGURE 3. Main process of drilling positioning control parameters determined by RBF neural network.

B. ACA-BASED DRILLING BOREHOLES SEQUENCE PLANNING

According to mine construction regulations, a series of boreholes should be arrange in roadway section in a certain way. The optimal drilling sequence is of great significance to improve the tunneling efficiency and reduce the energy consumption. Boreholes sequence planning methods based on minimum moving distance and minimum swing angle were proposed and compared. Equation (9) and equation (10) represent the optimization objectives of the two methods, respectively.

$$S = \sum_{i=1}^{n-1} l_i \quad (i = 1, 2, \cdots, n-1) \tag{9}$$

where S denotes the total moving distance of drilling-rod, l_i denotes the distance between two adjacent holes, and n is the number of boreholes.

$$J = \sum_{j=1}^{n-1} \left|\theta_j - \theta_{j+1}\right| \tag{10}$$

where J is the sum of all joint angles.

At present, algorithms commonly used in robot path planning mainly include A* algorithm, Dijkstra algorithm, Theta* algorithm and other complete algorithms with large complexity, as well as sampling-based planning algorithms such as RRT algorithm, RRT-connect algorithm and rolling online RRT algorithm (with wide application in high dimensions). In addition, there are artificial potential field method, BUG algorithm and incremental heuristic algorithm (LPA* algorithm, D* Lite algorithm), which are mainly used for motion control in high dynamic environment. The basic ant colony algorithm has high computational complexity and high cost of solving time and initializes a lot of parameters determined empirically.

Simple and reliable optimization algorithms is required for the path planning of drilling machines in mines. Based on comprehensive consideration of other path planning algorithms and the positioning characteristics of mining machinery, good communication between IPC (Industrial Personal Computer) and PLC ensures the application of ACA to control mining equipment. Ant colony algorithm (ACA) is adopted for arrayed boreholes sequence planning owing to its fast convergence and small cumulative error. ACA-based borehole sequence planning procedure is shown in Figure 4. Borehole sequence planning problem is expressed as a digraph with N points of $G = (N, A)$. Where $N = \{1, 2, \ldots, n\}$ and $A = \{(p, q)|p, q \in \mathrm{N}\}$.

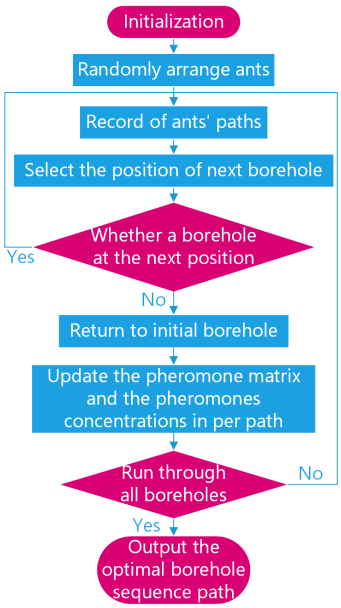

FIGURE 4. Borehole sequence planning procedure based on ACA.

The variable (distance or angle) between two holes is described as $(d_{pq})_{n\times n}$ and the objective function can be expressed as

$$f(w) = \sum_{i=1}^{n} d_{k_{i-1}k_i} \tag{11}$$

where $w = (k_1, k_2, \ldots, k_n)$ is a sequence of boreholes planning and k_i means the i-th borehole after sequence planning.

Random probability of boreholes selection and pheromone are the key parameters in ACA. Taking a borehole-positions as the initial point, the borehole sequence is stored by memory vector, and the next borehole is selected according to the

random probability, which is expressed in

$$P_{ij}^{k}(t)\begin{cases}\dfrac{[\tau_{ij}(t)]^{\alpha}\times[\eta_{ij}(t)]^{\beta}}{\sum\limits_{k\notin allowed_k}[\tau_{ik}(t)]^{\alpha}\times[\eta_{ik}(t)]^{\beta}} & j\in allowed_k\\ 0 & otherwise\end{cases}\tag{12}$$

where $\tau_{ij}(t)$ is the pheromone concentration between the initial point i and the termination point j, with the initial moment $\tau_{ij}(t) = Const$; $\eta_{ij} = 1/d_{ij}$ is volatile function indicating the pheromone visibility between two points; $allowed_k$ is a collection of unvisited points at time t, α and β are the pheromone inspired factor and the self-inspired factor characterizing the importance of pheromone concentration to the individual selection path of ants and the importance of visibility respectively.

As presented in (13), the pheromones on all paths will evaporate at a certain rate after each iteration.

$$\begin{cases}\tau_{ij}(t) = (1-\rho)\tau_{ij} + \sum\limits_{r=1}^{f}\Delta\tau_{ij}^{r}\\ \Delta\tau_{ij}^{r} = \begin{cases}(C_r)^{-1} & \text{Ant } r \text{ from } i \text{ to } j\\ 0 & \text{others}\end{cases}\end{cases}\tag{13}$$

where f is the number of ants, ρ is the volatility coefficient of pheromone, $\Delta\tau_{ij}^{r}$ is the pheromone left in the path from point i to point j of ant r, C_r is the total path traveled by ant r.

Based on the above theories, the specific ACA for drilling sequence planning was constructed. The computational complexity of the ACA model used in this article is shown in TABLE 2. Compared with basic ACA, it significantly reduces the calculation of path distance (or angle) and the complexity of parameter initialization.

TABLE 2. The computational complexity of the proposed model.

	The basic ACA	The ACA variant proposed in this article
Parameter initialization	$O(n^2+m)$	$O(n^2)$
Starting point selection	O(m)	O(m)
Path selection	$O(mn^2)$	$O(mn^2)$
Path distance calculation	$O(mn^2)$	O(mn)
Pheromone updating	$O(n^2)$	$O(n^2+mn)$
Clear the path record table and continue the iteration	O(mn)	O(mn)
Result outputing	O(1)	O(1)

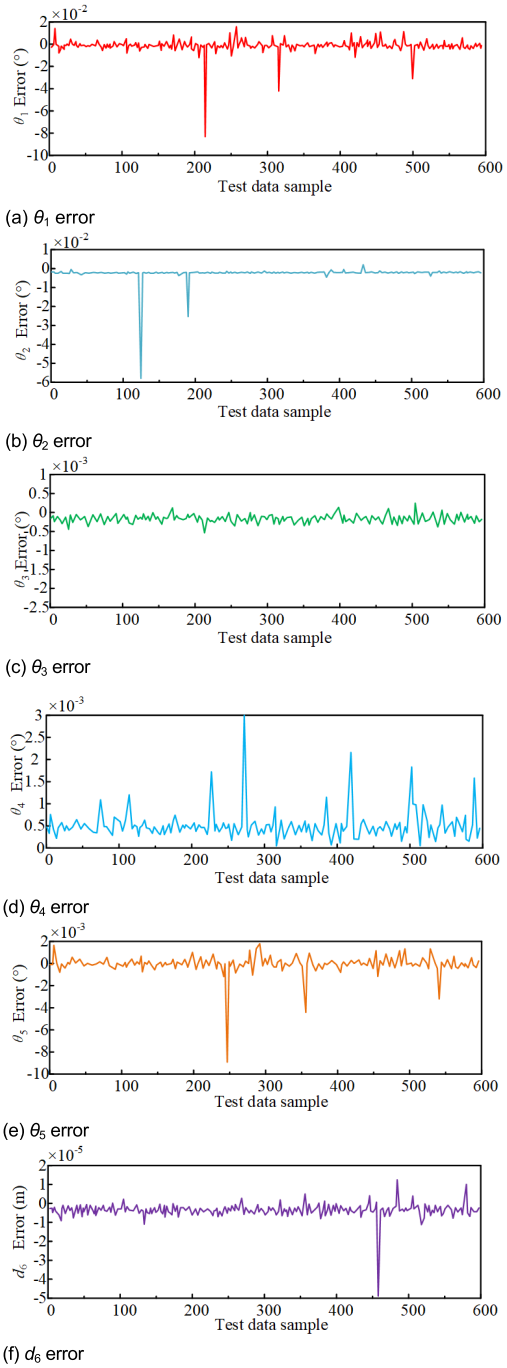

FIGURE 5. Prediction errors of joint variables.

IV. SIMULATION AND ANALYZATION

A. DRILLING-ROD POSITIONING SIMULATION

5400 groups of data are randomly generated in MATLAB toolbox for model training, and 600 groups were used for test. The true-value of each joint variable is obtained by RBF neural network. Errors shown in Figure 5 are obtained by comparing the test result and the true-value of each joint variable acquired by RBF neural network. It is easy to know that the maximum angle error does not exceed 0.01° (0.6%) while the maximum moving error is no more than 0.5mm.

25 boreholes were designed and arranged in a roadway section of 3m × 3.2m to test the borehole positioning simulation. Joint variables obtained by the RBF neural network algorithm are brought into the space model (8) to acquire the actual positions of drilling-rod shown in Figure 6. Position deviations of boreholes are shown in Figure 7 indicating that predicted borehole positions are basically coincident with the

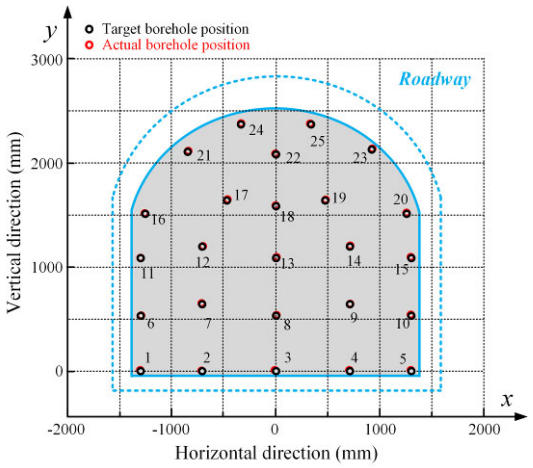

FIGURE 6. Simulation results of borehole positioning in roadway section.

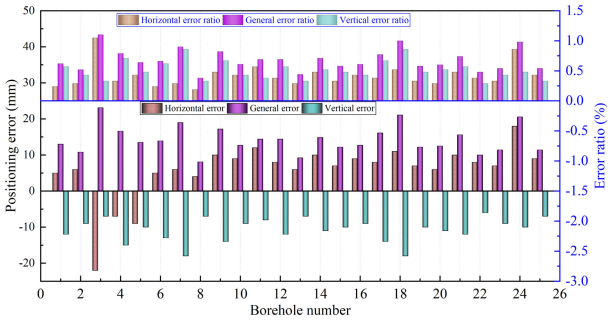

FIGURE 7. Error distributions of borehole positioning.

target position. In the simulation of 25 boreholes, the average error in x direction is 8.76mm while that is 10.72mm of y direction, and the general error is regulated below 1.1%. It is proved that the proposed borehole positioning method is feasible.

By the way, the error distribution also shows that the drilling mechanism easily produces over-damping control in the vertical direction, and the vertical-directional damping weight should be reduced in practical application.

B. BOREHOLES SEQUENCE PLANNING SIMULATION

1) PARAMETER OPTIMIZATION OF ACA

The efficiency and accuracy of boreholes sequence optimization are directly determined by the parameters of ACA, including the pheromone inspired factor α, the self-inspired factor β, and the volatilization factor ρ. The pheromone inspired factor α is set as 1, the self-inspired factor β is an integer selected at the range of 1 to 6, the volatilization factor ρ is a decimal number less than 1, respectively. The influence of different coefficients on minimum moving distance optimization results is explored and the envelope diagram of the optimal results under different parameters by interpolation is presented in Figure 8.

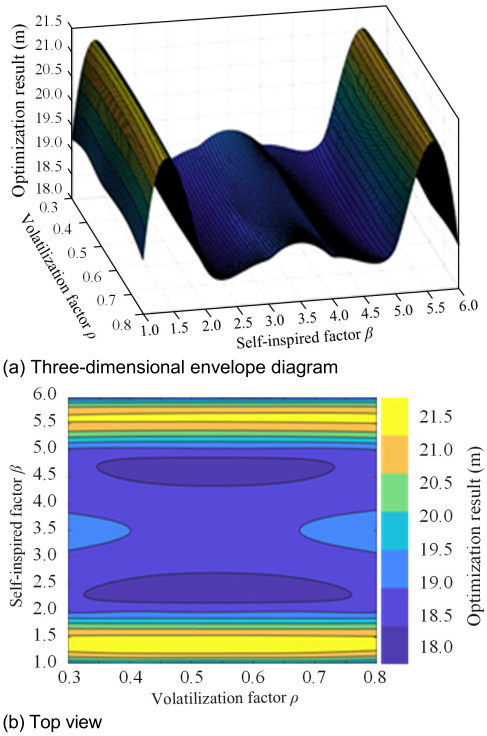

FIGURE 8. The envelope diagram under different parameters.

Best boreholes sequence planning optimization result appears at the pheromone volatilization factor ρ of 0.55 and the self-inspired factor β of 2.5.

2) SIMULATION RESULTS UNDER DIFFERENT OPTIMIZATION TARGETS

Based on optimal parameters obtained above, boreholes sequence planning simulation results under different optimization targets of minimum moving distance and minimum swing angle are shown in Figure 9.

In the simulation with the minimum moving distance as the optimization target, the total moving distance of the drilling-rod is 15900.32 mm, and the swing angle of the mechanism is 16.12 rad. In the optimization simulation aiming at the minimum swing angle, the total rotation angle of the mechanism is 15.25 rad (reduced by 5.4%), while the general moving distance is 16440.26 mm (increased by 3.4%). The ACA optimization with the minimum rotation angle improves the efficiency of drilling process and the convergence speed. The proposed scheme is beneficial to the control system of the drilling mechanism without the conversion of system parameters.

The iterations and running time of the optimizations of shortest moving distance and minimum swing angle of drilling rod are compared and analyzed, as shown in Figure 10 below. It can be found that the optimization of minimum swing angle increases the operating efficiency of the mechanism by 5.4% at the cost of 0.13% in running time.

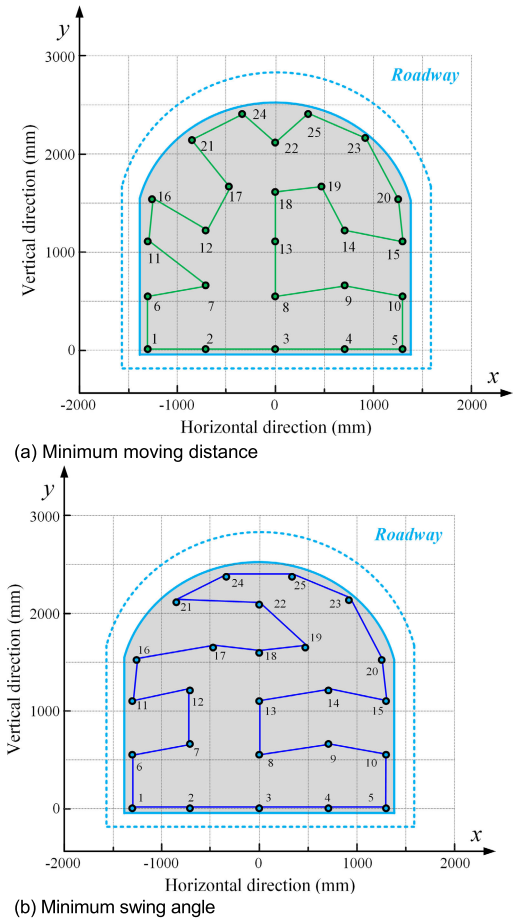

FIGURE 9. Boreholes sequence planning simulation results under different optimization targets.

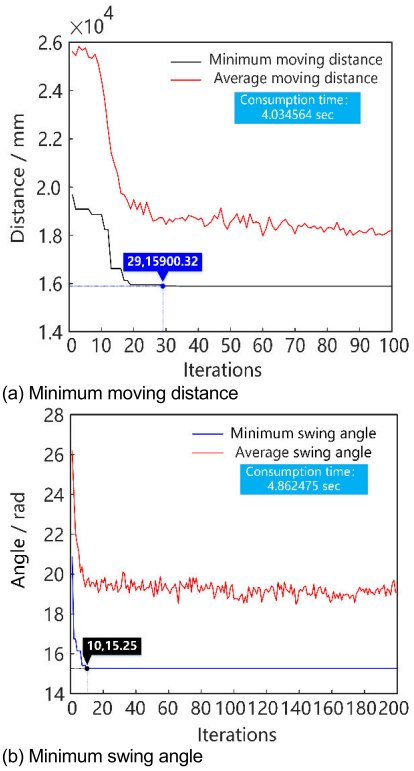

FIGURE 10. Computational costs under different optimization targets.

V. EXPERIMENTAL RESULTS AND DISCUSSIONS

A. EXPERIMENTAL BENCH

To verify the accuracy and feasibility of borehole positioning and sequence planning, experimental researches were carried out. Shown in Figure 11, drilling system, hydraulic control system, data processing system and data optimization center are the four parts of the experimental bench.

The test system consists of two PLC (CP1H) and six sensors, including five rotary encoders and one displacement sensor arranged in every joint. The hydraulic system is controlled by the slave PLC and directly drives the drilling-rod through the solenoid valves. Data optimization center is composed of OPC toolbox in Simulink and Kingview system, which realizes automatic real-time feedback control between MATLAB and PLC. The drilling system includes drilling jumbos, simulated roadway, sensors, and spraying mechanism. Ignoring the drilling time and the attitude adjusting process of drilling jumbos, a spraying mechanism was fixed to replace drilling-bit at the end of drilling-rod to research the drilling positioning technology.

The field test is a comprehensive environment with strong noise interference, which mainly includes machine vibration, electrostatic interference, magnetic interference and

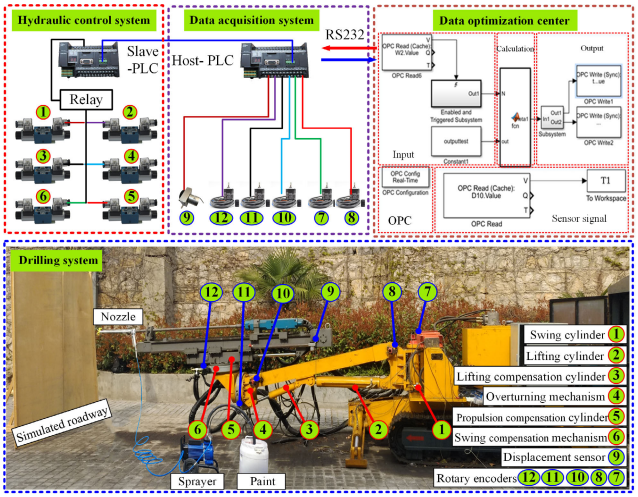

FIGURE 11. Experimental bench.

high-frequency electromagnetic interference. Firstly, all sensors are grounded, signals are transmitted by electrostatic shielded cables, and unnecessary cable connections (shown in Figure 12) are avoided. All the controllers are packed into a metal control cabinet to shield against high-frequency electromagnetic interference and remain isolated from the drilling jumbo to against vibration.

B. DRILLING-ROD POSITIONING TEST

In order to verify the accuracy of the drilling-rod positioning control algorithm, 10 boreholes were arranged in the

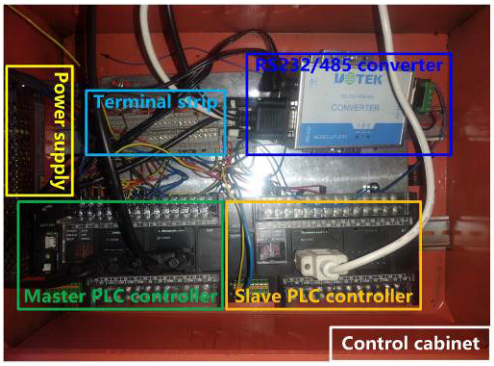

FIGURE 12. Experimental bench.

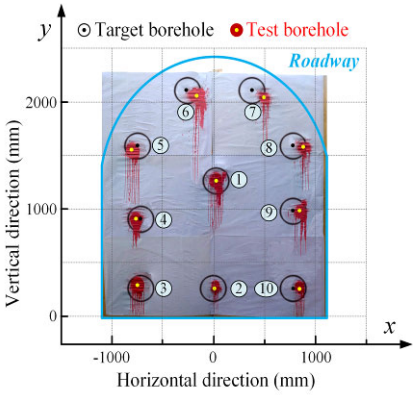

FIGURE 13. Borehole positioning test result.

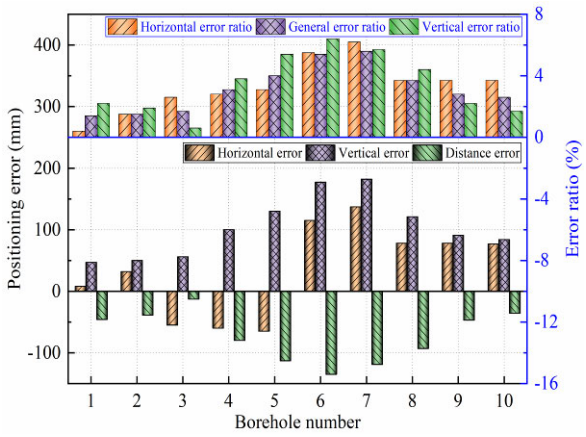

FIGURE 14. Experimental Borehole positioning error statistics.

simulated roadway section before the experiments. The positioning of drilling-rod was simulated on the drilling test system based on RBF neural network. Results of borehole positioning test are shown in Figure 13 and the positioning error analysis of the test is shown in Figure 14.

It can be seen that borehole 1 and borehole 2 have higher positioning accuracy while the general positioning errors become large at the top of roadway section (borehole 6 and borehole 7). Boreholes drilling on the left and right sides

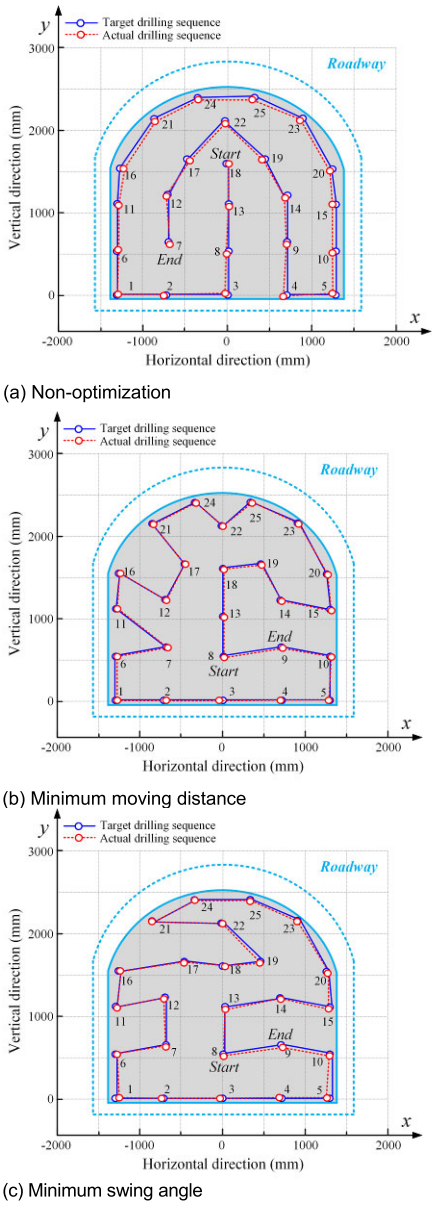

FIGURE 15. Boreholes sequence planning test results with different optimization targets.

of roadway section exceed the planned position, it is due to the assembly error of test equipment and the underdamping phenomenon appears in the adjustment in horizontal direction. In addition, the positioning error of the whole boreholes basically satisfies the normal distribution. As the statistics shows, the maximum positioning error is 5.6%, and the average positioning accuracy is 3.2%. The experiment indicates that RBF neural network can effectively achieve borehole drilling compensation with high precision.

C. BOREHOLES SEQUENCE PLANNING TEST

Reducing the movement path and time of drilling mechanism is one of the effective methods to improve the efficiency of drilling jumbo. The experimental researches were carried

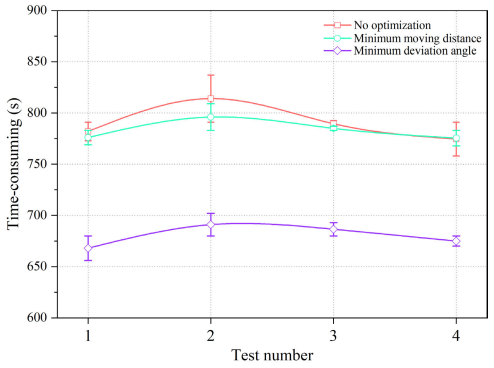

FIGURE 16. Drilling time of different boreholes sequence planning methods.

TABLE 3. Drilling time statistics of different boreholes sequence planning methods.

	Test 1(s)	Test 2(s)	Test 3(s)	Test 4(s)	Mean value (s)
Non-optimization	782	814	794	774.5	781.8
Minimum moving distance	776	796	785	775.5	777.7
Minimum swing angle	668	691	686.5	675	677.8

out with the optimization targets of non-optimization, minimum moving distance, and minimum swing angle. Driving cylinders of the drilling mechanism were set at constant speeds. Drilling time was selected as an indicator of the optimization result. Multiple tests were performed to prevent random errors from affecting the experimental results. Meanwhile, the experiment simulates the drilling operation only rather than actual drilling to avoid the influence of drilling time. Boreholes sequence planning test results are shown in Figure 15.

The conventional borehole drilling without optimization is more inclined to the horizontal and vertical drilling sequence. Drilling time statistical analysis was carried out to measure the efficiency of different borehole sequence planning methods and shown in TABLE 3 and Figure 16.

Obviously, boreholes sequence planning scheme with optimization target of minimum swing angle takes the least amount of total time. Due to the few number of boreholes in the test and relatively simple sequence planning, there is little difference in the consumed time between the non-optimization and the minimum distance optimization scheme. As shown in figure 12, the mean values of drilling time under non-optimization and minimum distance optimization are 16.3% and 15.1% larger than that of minimum swing angle optimization target, so as to the standard deviations, which indicates weakness in time-consuming of the two schemes. Therefore, aiming at the drilling sequence planning of multi-freedom mechanical arm driven by hydraulic cylinder, the minimum swing angle optimization scheme can reduce the traversal time and improve the traversal efficiency.

VI. CONCLUSION

In order to realize rapid tunneling in the hard-rock roadway, drilling-rod positioning and drilling sequence planning were investigated based on RBF neural network and ACA.

RBF neural network is used to control the positioning of drilling-rod. The simulation demonstrates that most of the predicted drilling-rod positioning are coincident with the target borehole positioning basically. The maximum error in horizontal direction is 22 mm while that is 18 mm in vertical direction, and the general error is controlled within 1.5%. And the experiment result indicates that the biggest position error ratio is 5.6% and the average positioning error of all holes is 104mm with error ratio of 3.2%. The computer simulation results are in good agreement with the experiment, which indicates the correctness of the method, and the overall error is basically controlled within the acceptable range of the project.

Ant colony algorithm (ACA) is adopted for drilling boreholes sequence planning and minimum swing angle optimization scheme for the manipulator is presented. It improves borehole traversal efficiency by 13.3% than that of non-optimization drilling method. Path planning with optimization target of minimum swing angle through Ant Colony Algorithm is a potential approach improving drilling efficiency of drilling mechanism.

REFERENCES

[1] Z. Jinzhu, "Rapid construction technology of large section tunnels by drill-blasting method," *Mod. Tunnelling Technol.*, vol. 15, no. 7, pp. 96–99, 2003.

[2] T. A. Sethu, T. P. Letsebe, and L. Magwaza, "Introduction of drill and blast utilizing pneumatic rock-drills in a Rwandan artisanal underground mine," *J. Southern Afr. Inst. Mining Metall.*, vol. 117, no. 4, pp. 313–319, 2017.

[3] H. Wang, W. Bao, T. Xu, and L. Song, "Study on coal mine fast drilling equipment and blasting key technology," in *Proc. 6th (ICEESD)*, Atlantis, CA, USA, 2017, pp. 26–30.

[4] X. Zhao, B. Huang, and Z. Wang, "Experimental investigation on the basic law of directional hydraulic fracturing controlled by dense linear multi-hole drilling," *Rock Mech. Rock Eng.*, vol. 51, no. 6, pp. 1739–1754, Jun. 2018.

[5] L. Songyong, C. Junfeng, and L. Xiaohui, "Rock breaking by conical pick assisted with high pressure water jet," *Adv. Mech. Eng.*, vol. 6, Jan. 2014, Art. no. 868041.

[6] F. Hamidi and A. Mortazavi, "A new three dimensional approach to numerically model hydraulic fracturing process," *J. Petroleum Sci. Eng.*, vol. 124, pp. 451–467, Dec. 2014.

[7] Y. Lu, S. Xiao, Z. Ge, Z. Zhou, Y. Ling, and L. Wang, "Experimental study on rock-breaking performance of water jets generated by self-rotatory bit and rock failure mechanism," *Powder Technol.*, vol. 346, pp. 203–216, Mar. 2019.

[8] I. W. Farmer and P. B. Attewell, "Rock penetration by high velocity water jet: A review of the general problem and an experimental study," *Int. J. Rock Mech. Mining Sci. Geomech. Abstr.*, vol. 2., no. 2, pp. 135–142, 1965.

[9] H. Jiang, C. Du, and K. Zheng, "Experimental research on the rock fragmentation loads of a water jetassisted cutting head," *Tehnicki Vjesnik/Tech. Gazette*, vol. 22, no. 5, pp. 1277–1286, 2015.

[10] Y. Xue, H. Si, D. Xu, and Z. Yang, "Experiments on the microscopic damage of coal induced by pure water jets and abrasive water jets," *Powder Technol.*, vol. 332, pp. 139–149, Jun. 2018.

[11] Y. Lu, S. Xiao, Z. Ge, Z. Zhou, and K. Deng, "Rock-breaking properties of multi-nozzle bits for tree-type drilling in underground coal mines," *Energies*, vol. 9, no. 4, p. 249, 2016.

[12] R. Ciccu and B. Grosso, "Improvement of disc cutter performance by water jet assistance," *Rock Mech. Rock Eng.*, vol. 47, no. 2, pp. 733–744, Mar. 2014.

[13] T. Stoxreiter, A. Martin, D. Teza, and R. Galler, "Hard rock cutting with high pressure jets in various ambient pressure regimes," *Int. J. Rock Mech. Mining Sci.*, vol. 108, pp. 179–188, Aug. 2018.

[14] M. Haddad and K. Sepehrnoori, "XFEM-based CZM for the simulation of 3D multiple-cluster hydraulic fracturing in quasi-brittle shale formations," *Rock Mech. Rock Eng.*, vol. 49, no. 12, pp. 4731–4748, Dec. 2016.

[15] O. Stephansson, H. Semikova, G. Zimmermann, and A. Zang, "Laboratory pulse test of hydraulic fracturing on granitic sample cores from Äspö HRL, sweden," *Rock Mech. Rock Eng.*, vol. 52, no. 2, pp. 629–633, Feb. 2019.

[16] C. Jiang-Zhan, C. Han, and S. Ping-He, "Mechanisms of fracture extending in coal rock by pulse hydraulic fracturing under triaxial loading" *Rock Soil Mech.*, vol. 38, no. 4, pp. 1023–1031, 2017.

[17] T. H. Yang, L. C. Li, L. G. Tham, and C. A. Tang, "Numerical approach to hydraulic fracturing in heterogeneous and permeable rocks," *Key Eng. Mater.*, vols. 243–244, pp. 351–356, Jul. 2003.

[18] P. Yuan and Y. Xu, "Experimental study on unloading effect of drill and blast excavation in high axial geostress," *Fresenius Environ. Bull.*, vol. 28, no. 11, pp. 7795–7802, 2019.

[19] W. Guo, Y. Wang, Z. Sun, and Q. Cai, "Smooth blasting technology in mine rock roadway under microscope technology," *Acta Microscopica*, vol. 28, no. 5, pp. 1108–1117, 2019.

[20] S. Chen, A. Wu, Y. Wang, X. Chen, R. Yan, and H. Ma, "Study on repair control technology of soft surrounding rock roadway and its application," *Eng. Failure Anal.*, vol. 92, pp. 443–455, Oct. 2018.

[21] Y. Wang, C. Fang, Q. Jiang, and S. N. Ahmed, "The automatic drilling system of 6R-2P mining drill jumbos," *Adv. Mech. Eng.*, vol. 7, no. 2, Feb. 2015, Art. no. 504861.

[22] W. R. Wu and J. Shi, "Down-the-Hole drill position based on mechanical mechanics and binocular stereo vision," *Adv. Mater. Res.*, vol. 908, pp. 291–295, Mar. 2014.

[23] Y. Zhang, J. Shao, D. Sun, X. Li, and N. Zhang, "Study on location parameter adjusting system for anchor drilling in coal mine roadways," in *Proc. IEEE 4th Inf. Technol. Mechatronics Eng. Conf. (ITOEC)*, Dec. 2018, pp. 1159–1162.

[24] T. Pirinen, J. Lassila, M. Loimusalo, J. Pursimo, and S. Hanski, "Automatic positioning and alignment for hole navigation in surface drilling," in *Proc. 31st Int. Symp. Autom. Robot. Construct. Mining (ISARC)*, Jul. 2014, vol. 31, no. 1.

[25] K. Andersson, "Simulation of a tunnel drilling sequence to determine loads on a rock drilling equipment," in *Proc. ADAMS User Conf.*, Rome, Italy, 2000, pp. 1–11.

[26] W. Wu and J. Yin, "Bore sequence planning of a three-arm rock-drilling rig," *J. Hefei Univ. Technol. (Natural Sci.)*, vol. 36, no. 2, pp. 149–151 and 207, 2013.

[27] Z.-Y. Chen and R. J. Kuo, "Combining SOM and evolutionary computation algorithms for RBF neural network training," *J. Intell. Manuf.*, vol. 30, no. 3, pp. 1137–1154, Mar. 2019.

[28] H.-G. Han and J.-F. Qiao, "Adaptive computation algorithm for RBF neural network," *IEEE Trans. Neural Netw. Learn. Syst.*, vol. 23, no. 2, pp. 342–347, Feb. 2012.

[29] M. Awad, "Forecasting of chaotic time series using RBF neural networks optimized by genetic algorithms," *Int. Arab Inf. Technol.*, vol. 14, no. 6, pp. 826–834, 2017.

[30] N. Arana-Daniel, A. A. Gallegos, C. López-Franco, and A. Y. Alanis, "Smooth global and local path planning for mobile robot using particle swarm optimization, radial basis functions, splines and Bézier curves," in *Proc. IEEE Congr. Evol. Comput. (CEC)*, Jul. 2014, pp. 175–182.

[31] J. Chen, P. Zhao, H. Liang, and T. Mei, "Motion planning for autonomous vehicle based on radial basis function neural network in unstructured environment," *Sensors*, vol. 14, no. 9, pp. 17548–17566, 2014.

[32] T. Chettibi, "Smooth point-to-point trajectory planning for robot manipulators by using radial basis functions," *Robotica*, vol. 37, no. 3, pp. 539–559, Mar. 2019.

[33] Z. Masoumi, J. V. Genderen, and A. S. Niaraki, "An improved ant colony optimization-based algorithm for user-centric multi-objective path planning for ubiquitous environments," *Geocarto Int.*, 2019, pp. 1–33, doi: 10.1080/10106049.2019.1595176.

[34] H. Yang, J. Qi, Y. Miao, H. Sun, and J. Li, "A new robot navigation algorithm based on a double-layer ant algorithm and trajectory optimization," *IEEE Trans. Ind. Electron.*, vol. 66, no. 11, pp. 8557–8566, Nov. 2019.

[35] G. Che, L. Liu, and Z. Yu, "An improved ant colony optimization algorithm based on particle swarm optimization algorithm for path planning of autonomous underwater vehicle," *J. Ambient Intell. Humanized Comput.*, pp. 1–6, 2019, doi: 10.1007/s12652-019-01531-8.

[36] A. Jayaprakash and C. KeziSelvaVijila, "Feature selection using ant colony optimization (ACO) and road sign detection and recognition (RSDR) system," *Cognit. Syst. Res.*, vol. 58, pp. 123–133, Dec. 2019.

[37] M. G. H. Omran and S. Al-Sharhan, "Improved continuous ant colony optimization algorithms for real-world engineering optimization problems," *Eng. Appl. Artif. Intell.*, vol. 85, pp. 818–829, Oct. 2019.

[38] C. Mu, J. Zhang, Y. Liu, R. Qu, and T. Huang, "Multi-objective ant colony optimization algorithm based on decomposition for community detection in complex networks," *Soft Comput.*, vol. 23, no. 23, pp. 12683–12709, Dec. 2019.

[39] Y. Zhao, W. Li, X. Wang, and C. Yi, "Path planning of slab library crane based on improved ant colony algorithm," *Math. Problems Eng.*, vol. 2019, Aug. 2019, Art. no. 7621464.

[40] X. Dai, S. Long, Z. Zhang, and D. Gong, "Mobile robot path planning based on ant colony algorithm with A* heuristic method," *Frontiers Neurorobot.*, vol. 13, pp. 1–15, Apr. 2019.

[41] L. Yue and H. Chen, "Unmanned vehicle path planning using a novel ant colony algorithm," *EURASIP J. Wireless Commun. Netw.*, vol. 2019, no. 1, pp. 1–9, Dec. 2019.

YUMING CUI (Member, IEEE) was born in Xuzhou, Jiangsu, China, in 1988. He received the Master of Engineering degree in mechanical design and theory from the China University of Mining and Technology, Xuzhou, Jiangsu, China, in 2015, where he is currently pursuing the Ph.D. degree in mechatronic engineering.

His research interests include intelligent tunneling and hard rock fragmentation method.

SONGYONG LIU was born in Shijiazhuang, Hebei, China, in 1981. He received the Ph.D. degree in mechanical design and theory from the China University of Mining and Technology, Xuzhou, Jiangsu, China, in 2009.

Since 2015, he has been a Professor with the School of Mechatronic Engineering, China University of Mining and Technology. He is the author of two books, more than 50 articles, and more than 76 inventions. His research interests include design and dynamics of excavation machinery, and rock breaking assisted with water jet.

HUIFU JI received the B.S. degree from the China University of Mining and Technology, Xuzhou, Jiangsu, China, in 2012, where he is currently pursuing the Ph.D. degree in mechanical design and theory.

His research interests include hydraulic system control and automation technology.

YUHUI HAN was born in Hebei, China, in 1993. He received the Master of Engineering degree in mechanical design and theory from the China University of Mining and Technology, in 2019.

His research interests include industrial automation technology and intelligent manufacturing.

YUESHEN YU received the Master of Engineering degree in control theory and control engineering, in 2004, and the Ph.D. degree in electrical engineering from the China University of Mining and Technology, Xuzhou, Jiangsu, China, in 2012.

Since 2013, he has been an Assistant Professor with the School of Electrical and Power Engineering, China University of Mining and Technology. His research interests include electrical explosion protection technology and industrial automation technology.